CHEMICAL ENGINEERING TRANSACTIONS
VOL. 70, 2018

A publication of AIDIC
The Italian Association of Chemical Engineering
Online at www.aidic.it/cet

Guest Editors: Timothy G. Walmsley, Petar S. Varbanov, Rongxin Su, Jiří J. Klemeš

ISBN 978-88-95608-67-9; **ISSN** 2283-9216

DOI: 10.3303/CET1870102

Numerical Study of Competition Effects of Laser Parameters on a Transient Melt Pool Evolution Process

Qingfei Bian, Xiaoli Tang, Renkun Dai, Qiuwang Wang, Min Zeng*

Key Laboratory of Thermo-Fluid Science and Engineering, Ministry of Education, School of Energy and Power Engineering, Xi'an Jiaotong University, Xi'an 710049, China
zengmin@mail.xjtu.edu.cn

The melt pool, formed by the superheated molten metal, is the initiation of solid part and the general process of laser additive manufacture process. The transient phenomena in the melt pool are of paramount interest in obtaining an optimum mechanical performance. In this paper, the different transient evolution phenomena of melt pool for the moving and fixed laser beam during the laser irradiation process are investigated, then the quantitative competition effects of the laser parameters on those transient phenomena are also studied. The results show that the evolution of melt pool gradually enters into the quasi-steady-state for the moving laser condition, the deformation of free surface almost has no change near the forward of laser beam. However, the fixed laser condition has different evolution process and the deformation of free surface becomes larger and larger even piercing the workpiece. The melt pool evolution becomes vigorous and prone to enter the quasi-steady-state with the increasing energy input per unit area which directly dominated by the laser parameters. Further investigation on the quantitative percentage of each parameter on the evolution shows that the laser scan speed is the most important factor for the evolution of melt pool.

1. Introduction

Laser-based additive manufacture (LBAM) technique, characterized by flexibility, rapid fabrication and layer-wise cladding, based on a computer aided design (CAD) data (Li et al., 2005) which can be used for a variety of industrial applications, such as laser aided deposition, part repair, surface hardening and welding (Han et al., 2005). The melt pool, as the general and important process of the LBAM which formed by the superheated molten metal, is the initiation of the solid part (Hua et al., 2008). The transient phenomena in the melt pool including the morphology of the free surface, thermodynamic evolution and melt pool dimension are of paramount interest in obtaining an optimum mechanical performance (Thompson et al., 2015). The laser parameters are the common factors, which directly decided the energy input per unit area of the melt pool and attracted the focus by many researchers on improving the evolution process of those phenomena. Wang et al. (2008) numerically revealed that the cooling rate at the liquid/solid interface decreased as the laser power increased and the scan speed decreased, which significantly affected the quality of resultant product. Li et al. (2005) studied the effect of the input power on the melt pool formation, they found that with increasing input power the dimension of the deposition layer increased. Pi et al. (2011) studied the melt pool evolution process using different laser diameters and found when the laser diameter increased the melt pool evolution became inactive. Fathi et al. (2014) demonstrated that the melt pool dimension was parabolic dependence on laser scan speed. However, most of the literatures concentrate on the effects of the laser parameters on the inner evolution of melt pool, such as the melt pool dimension, the solidification/melting interface shape and the dynamics of the melt pool. Few literatures pay attentions to the evolution of the free surface of the melt pool, which also has been proved to have important effects. The study of the surface deformation evolution can help us understand the actual evolution mechanism of the melt pool. Besides, the laser parameters have significant effect on the melt pool evolution and researchers have great interest in adjusting which to control the melt pool evolution, however, the competition effects of the parameters are not clearly clarified, the exploration of which can give us a guidance about adjusting what parameter on control of the melt pool evolution in practice.

Please cite this article as: Bian Q., Tang X., Dai R., Wang Q., Zeng M., 2018, Numerical study of competition effects of laser parameters on a transient melt pool evolution process , Chemical Engineering Transactions, 70, 607-612 DOI:10.3303/CET1870102

Therefore, in this paper a more comprehensive investigation on the evolution phenomena of melt pool, including not only the inner phenomena but also the important free surface deformation, for both the moving and fixed laser beam during the laser irradiation process are carried out using a numerical model developed by Bian et al. (2017). Then the effects of the laser parameters on those transient phenomena of the melt pool are studied and the quantitative competition influence percentage of them is lastly obtained based on the Taguchi method deduced by Taguchi et al. (1987).

2. Model establishment

The whole 2D physical model, consisting of workpiece, protecting gas, laser beam and melt pool, is illustrated in Figure 1a. The dimension of the model is 10 mm×10 mm, the top-half is protecting gas and the bottom is workpiece. When the laser irradiates on the surface of workpiece, the workpiece is quickly overheated and melt, a pool emerges beneath the laser center. Between the melt pool and the solid workpiece, there is a region named mushy region in which both of the metal liquid and dendritic solid exist and the solidification/melting process occurs frequently. The surrounding for the workpiece is the inert gas region which is used to protect the high temperature metal from the chemical reaction. The detail thermal dynamic among the four regions during the evolution process of the melt pool is shown in Figure 1b.

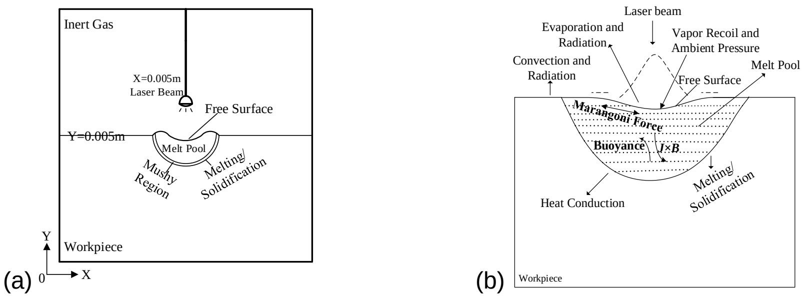

Figure 1: The schematic 2D physical melt pool model (a) physical model; (b) Thermal dynamic in melt pool

2.1 Basic assumptions and Mathematic model

On the basis of accuracy in simulation, some assumptions which include the laser beam profile is assumed as Gaussian distribution, the fluid flow is assumed to be laminar and incompressible and the Boussinesq approximation is used to describe the buoyancy driven flow, are made to make the model simplified and tractable. The governing equations are expressed in the following form:

$$\frac{\partial \rho}{\partial t}+\frac{\partial \rho u}{\partial x}+\frac{\partial \rho v}{\partial y}=0 \tag{1}$$

$$\frac{\partial(\rho u)}{\partial t}+\nabla(\rho\vec{v}u)=\nabla(\mu \mathrm{grad}u)-\frac{\partial P}{\partial x}-\frac{K_0(1-g_l)^2}{g_l^{\,3}+\zeta}u \tag{2}$$

$$\frac{\partial(\rho v)}{\partial t}+\nabla(\rho\vec{v}v)=\nabla(\mu \mathrm{grad}v)-\frac{\partial P}{\partial y}-\frac{K_0(1-g_l)^2}{g_l^{\,3}+\zeta}v+\rho g\beta(T-T_0) \tag{3}$$

$$\frac{\partial(\rho h)}{\partial t}+\nabla(\rho\vec{v}h)=\nabla(\lambda \mathrm{gradT})-\frac{\partial(\rho\Delta H g_l)}{\partial t}+\mathrm{div}(\rho\vec{v}\Delta H g_l) \tag{4}$$

Where ρ, u, v, P, μ, T, λ and h are density, velocity, pressure, fluid viscosity, temperature, thermal conductivity and enthalpy, respectively. K_0 is a permeability coefficient and ζ is a small number. g_l is the liquid fraction. The definition of VOSET method (Sun et al., 2010) is shown as the following equations:

$$\frac{\partial C}{\partial t}+\nabla(\vec{v}C)=0, \vec{n}=\nabla\phi/|\nabla\phi|;\ Where\ \phi=-d, if\ \mathrm{C}_{i,j}>0.5;\ 0, if\ \mathrm{C}_{i,j}=0.5\ and\ d, if\ \mathrm{C}_{i,j}<0.5 \tag{5}$$

Where C is the volume fraction, ϕ is the level set function, the d is the shortest distance from grid point (i, j) to interfaces and the precise normal vector is reconstructed by the signed distance function. Based on the CSF (Continuum Surface Force) model, the momentum boundary conditions and the energy boundary condition are expressed as follows:

$$Q = \left(\frac{2\eta P_{laser}}{\pi R^2}\exp\left(-\frac{2r^2}{R^2}\right) - \varepsilon\sigma(T^4 - T_\infty^4) - \rho_l V_0 \exp(-U/T_{surf})L_v\right)\delta(\phi) \quad (6)$$

$$F_n = (AB_0 T_{surf}^{-1/2}\exp(-U/T_{surf}) + \gamma\nabla\vec{\mathbf{n}}\nabla(\phi))\delta(\phi);\ and\ F_t = -\frac{d\gamma}{dT}\nabla(T)\delta(\phi) \quad (7)$$

Where V_0 is the sound velocity in melt pool and a value of 3,500 m/s is utilized in this study. U is the heat of evaporation per Avogadro's number atoms. $\delta(\phi)$ is the derivative of the Heaviside function. A is the ambient pressure dependent coefficient. B_0 is the evaporation constant.

2.2 Numerical implementation and model validation

In present study, the governing equations are solved by the SIMPLE algorithm which are discretized based on the finite volume method (FVM), the convection term is solved by high order MUSCL scheme and the central difference is used for the diffusion term. The second order projection method is adopted in the solution procedure of VOSET method (Tao, 2001). To obtain a grid independency solution, four different grids (50×50, 100×100, 150×150 and 200×200) are studied and finally the uniform grid 150×150 is selected for such numerical investigations as presented in Figure 2a. To validate the accuracy of our developed model for the simulation in melt pool, a comparison with Han's investigation (Han et al., 2005) is made firstly. Figure 2b presents the comparison of the temperature distribution of the workpiece/inert gas interface along the x-axis between present work and Han's simulation at 2 ms, it found obviously that they coincide very well. However, the dimension of the melt pool in present simulation is slight larger compared with Han's experiment as shown in Figure 3. The mean absolute errors of the dimension for the fixed and moving laser beam are 0.07 mm and 0.09 mm, respectively, and the corresponding mean relative errors are 9.5 % and 11.3 %. The test results illustrate that the present simulation method of the flow and heat transfer in melt pool is convincible and acceptable.

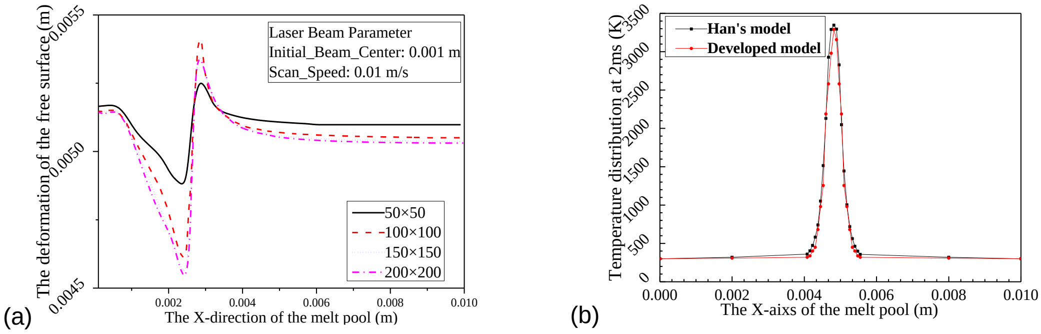

Figure 2: (a) The grid independency test. (b) Validation of the temperature distribution

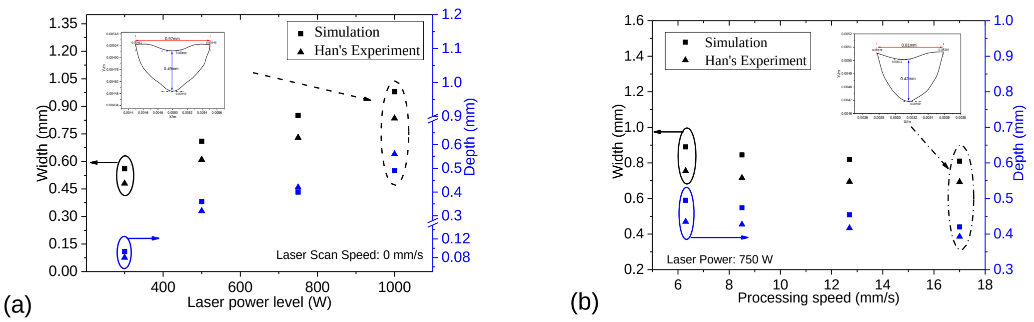

Figure 3: Validation of the melt pool dimension

3. Results and Discussion

3.1 The transient phenomena during the evolution of the melt pool

To study the transient phenomena during the evolution of the melt pool, two cases have been simulated in this section. The laser beam in Case 1 is moved with a scan speed 0.01 m/s while that in Case 2 is fixed. It found that the transient phenomena of the free surface of melt pool in two cases are significantly different even though they are irradiated by same power laser beam as exhibited in Figure 4. In Case 1 (Figure 4a), the deformation of the free surface, the keyhole called in some literatures, becomes larger (the hollow becomes deeper and the hump becomes higher) during the early stage of the laser scanning process and reaches a critical state at 150 ms, and then the evolution of the free surface presents a quasi-steady-state (the hump and the hollow almost have no change near the forward of the laser beam from 150 ms to 300 ms). However, in Case 2 (Figure 4b), the deformation of the free surface becomes larger and larger with the power input until the workpiece is pierced by the laser beam (this phenomenon is common in the welding pool).

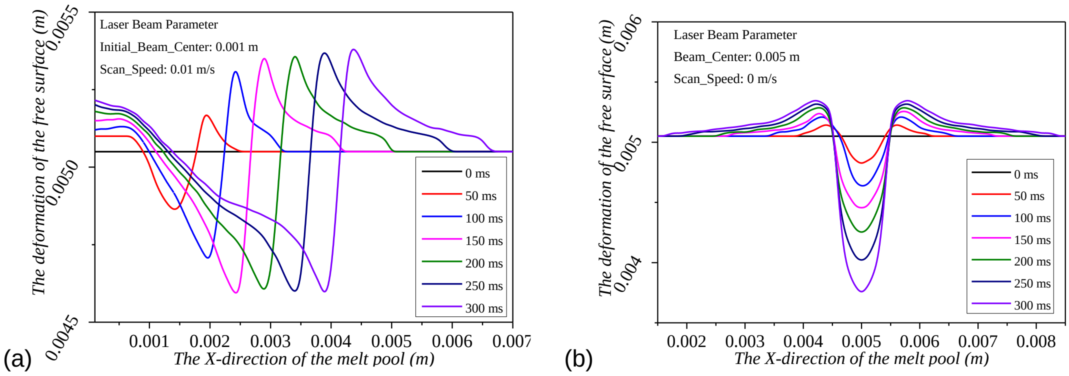

Figure 4: Shapes of the free surface versus times (a) Moving laser beam, (b) Fixed laser beam

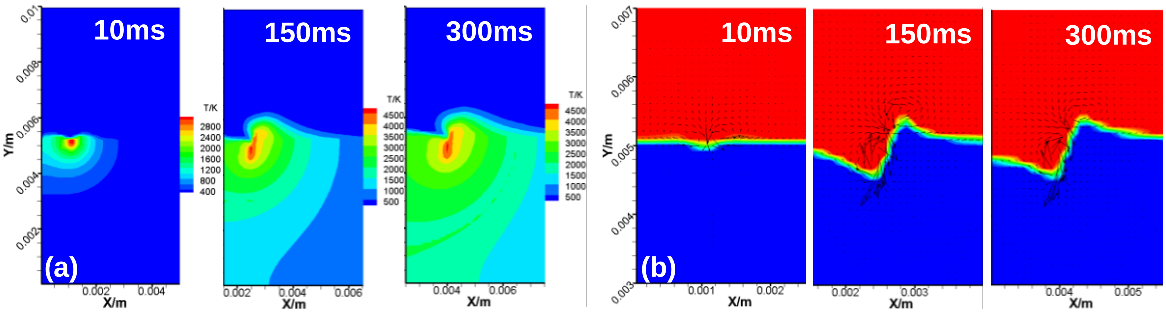

Figure 5: Contours of the velocity (a) and temperature (b) distribution versus times

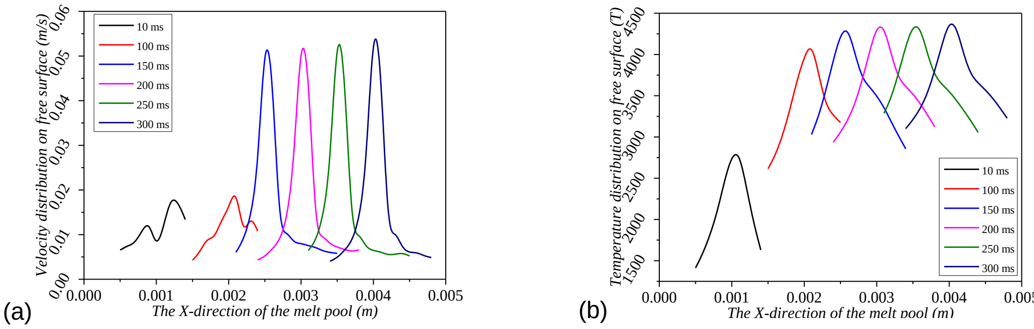

Figure 6: Velocity (a) and temperature (b) distribution on the free surface versus times

Figure 6 shows the temperature distribution in the zone at various times in Case 1. Before the evolution of the melt pool approaches the critical time (150 ms), the peak temperature near the free surface increases continuously (the value of which at 10 ms is 2,800 K and it reaches to 4,500 K at 150 ms). Until entering the quasi-steady stage, the peak temperature of the melt pool remains around 4,500 K. The velocity of the melt pool and surrounding inert gas near the free surface have analogous evolution procedure as the peak temperature. As shown in Figure 6, the velocity increases sharply during the period from 10 ms (0.002 m/s) to 150 ms (0.055 m/s) while the velocity almost has no change and the peak value keeps at 0.055 m/s after 150 ms. The detailed velocity and temperature distribution on the free surface near the forward of the laser beam at various times are also presented in Figure 7. It’s clearly observed that the velocity and temperature profiles versus time remain the same morphology after 150 ms, which means both the energy and the momentum on the free surface near the laser beam forward reach balance in that moment.

It is common knowledge that the convection motion in melt pool would be from high temperature zone to low temperature zone under the driven by the Marangoni convection induced by a negative surface tension temperature gradient. Thus, in our study the metal liquid in melt pool will transport from laser center to the pool periphery building the hollow in laser center and hump in the edge. With the rightward moving of the laser center, the hollow of the free surface moves toward right correspondingly and the hump also advances to right driven by the rightward Marangoni convection (from the beam center to right periphery). At the same time, the old hollow which is the position of the previous beam center, is filled by the leftward Marangoni convection (from the new center to left periphery). This process continues all the time during the scanning of the laser beam and the free surface (keyhole) gradually shapes. While the energy and the momentum near the beam center reach balance, and then the above ‘advanced and filled’ process also reaches balance. Hence the free surface morphology changes little after then and the melt pool evolution enters the quasi-steady stage. Since the temperature of the irradiated point is always higher than other points owing to the fixed location of the irradiated point along the X-axis in Case 2, the liquid metal always transports toward the periphery of the melt pool from the beam center under the driving of the Marangoni convection. The hollow located at beam center becomes deeper and deeper and the surrounding hump gets higher and higher until the workpiece is pierced.

Table 1: Levels of each factor in this study

Code	Factors (unit)	Level 1	Level 2	Level 3
A	Laser scan speed (m/s)	0.01	0.015	0.02
B	Laser spot diameter (m)	0.0006	0.0005	0.0007
C	Laser power (W)	80	100	120

Table 2: The orthogonal test and results

No. i	A	B	C	Test results Y_i (mm)			
				MPD		FSD	
				depth	width	hollow	hump
1	1	1	1	3.0	6.2	4.6	5.4
2	1	2	2	5.5	10.0	4.0	5.5
3	1	3	3	5.3	7.4	4.5	5.4
4	2	1	2	4.5	6.3	4.6	5.3
5	2	2	3	5.4	7.8	4.2	5.4
6	2	3	1	2.7	5.7	4.8	5.3
7	3	1	3	3.6	6.0	4.7	5.3
8	3	2	1	2.5	5.7	4.7	5.3
9	3	3	2	1.8	5.3	4.9	5.2

3.2 Parametric analysis by Taguchi method

It’s obvious that the three parameters, the laser scan speed, the laser power and the laser spot diameter, play foremost roles in the evolution process of the melt pool in above study. In order to clarify the effect of each parameter quantitatively, the advantageous Taguchi method (Taguchi et al., 1987) is used in our study. The control factors and the level of each factor in this study are shown in Table 1. Then the orthogonal test design is established and the related results (Y_i) of the melt pool dimension (MPD) and the free surface deformation (FSD) are also obtained as shown in Table 2.

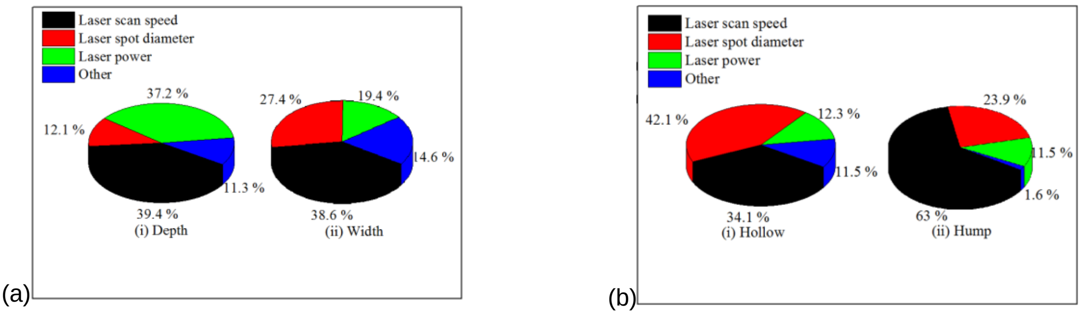

Figure 7: Percentage of each parameter on the melt pool dimension (a) dimension; (b) surface deformation

The factor fluctuation variance S_f, the error fluctuation variance S_e and the quantitative percentage of each parameter ϑ_j can be calculated by following formula based on the numerical database:

$$S_f = \sum_{m=1}^{3}(\sum_{Level\ m} Y_i)^2 \Big/ 3, S_e = (\sum_{i=1}^{9} Y_i^2 - (\sum_{i=1}^{9} Y_i)^2 \Big/ 9 - \sum_{f=A}^{C} S_f) \Big/ f_e, \vartheta_f = (S_f - S_e) \Big/ (\sum_{i=1}^{9} Y_i^2 - (\sum_{i=1}^{9} Y_i)^2 \Big/ 9) \quad (8)$$

where *f* represents the factor *A*, *B* and *C*, respectively; *m* denotes the level of each factor. The f_e is the degree of freedom of error and a value of 2 is obtained in this study.

Figure 7 shows the percentage of each parameter effects on the evolution of the melt pool. It found that the laser scan speed has the largest effect on the dimension of the melt pool, while the laser power and laser spot diameter take the second place in the evolution of the depth and width, respectively (Figure 7(a)). For the free surface shape, the laser spot diameter and laser scan speed dominate the evolution of the hollow and hump, however, the laser power has small influence on the free surface of the melt pool (Figure 7(b)).

4. Conclusions

In this paper the different transient evolution phenomena of melt pool for the moving and fixed laser beam during the laser irradiation process are investigated and analysed using a developed multiphase model. Then the effects of the laser parameters on those transient phenomena are studied and the quantitative competition influence percentage of them is obtained by the Taguchi method. The main conclusions can be drawn as follows:

(1) The deformation of the free surface, the temperature and velocity of the melt pool initially increase for both the moving and fixed laser beam. After then the evolution of melt pool enters into the quasi-steady-state for the moving laser condition, during that period the shape of free surface, the velocity and temperature on the free surface near the laser change slightly. However, the fixed laser condition has different evolution process, the deformation of the free surface becomes larger and larger even piercing the workpiece.

(2) Further study on the quantitative competition effect of each parameter on the evolution of the melt pool shows that the melt pool evolution is dominated by the lasers parameters. The laser scan speed is proved to be the most important factor during the evolution of melt pool, and the other two parameters, laser spot diameter and laser power, take second place in evolution of the free surface and the melt pool dimension, respectively.

Acknowledgments

This present study is financially supported by the National Natural Science Foundation of China (Grant No. 51776157).

References

Han L., Liou F.W., Musti S., 2005, Thermal behaviour and geometry model of melt pool in laser material process, Journal of Heat Transfer, 127(9), 1005-1014.

Hua T., Jing C., Xin L., 2008, Research on molten pool temperature in the process of laser rapid forming, Journal of Materials Processing Technology,198(1), 454-462.

Thompson S. M., Bian L., Shamsaei N., 2015, An overview of direct laser deposition for additive manufacturing; part i: transport phenomena, modeling and diagnostics, Additive Manufacturing, 8, 36-62.

Wang L., Felicelli S., Gooroochurn Y., 2008, Optimization of the LENS ® process for steady molten pool size, Materials Science & Engineering A, 474(1–2), 148-156.

Li P., Yang T., Li S., 2005, Direct laser fabrication of nickel alloy samples, International Journal of Machine Tools & Manufacture, 45(11), 1288-1294.

Pi G., Zhang A., Zhu G., 2011, Research on the forming process of three-dimensional metal parts fabricated by laser direct metal forming, International Journal of Advanced Manufacturing Technology, 57(9), 841-847.

Fathi A., Mozaffari A., 2014, Vector optimization of laser solid freeform fabrication system using a hierarchical mutable smart bee-fuzzy inference system and hybrid map, Journal of Intelligent Manufacturing, 2, 775-795.

Bian Q.F., Dai R. K., Tang X.L., Liu Q., Wang Q.W., Zeng M., 2017, Investigation on the effect of the thermal dynamic, evaporation and alternative material properties with a developed 2D model based on the VOSET method. Numerical Heat Transfer, 83, 204-221.

Sun D.L., Tao W.Q., 2010, A coupled volume-of-fluid and level set (VOSET) method for computing incompressible two-phase flows, International Journal of Heat & Mass Transfer, 53(4), 645-655.

Tao W.Q., 2003, Numerical heat transfer, 2nd ed., Xi'an Jiao Tong University Press, Xi'an, China. (in Chinese)

Taguchi G., Konishi S., 1987, Orthogonal arrays and linear graphs, American Supplier Institute, Dearborn, US.

Zhao X., Iyer A., 2017, Numerical modeling of the thermal behaviour and residual stress in the direct metal laser sintering process of titanium alloy products. Additive Manufacturing, 1, 1-11.